

## Potential of perfusion imaging with IVIM MRI in breast cancer

Mami Iima<sup>1</sup>, Masako Kataoka<sup>1</sup>, Denis Le Bihan<sup>2</sup>, Masaki Umehana<sup>3</sup>, Takuma Imakita<sup>3</sup>, Masayuki Nakagawa<sup>1</sup>, Shotaro Kanao<sup>1</sup>, Kojiro Yano<sup>1,4</sup>, Thorsten Feiweier<sup>5</sup>, and Kaori Togashi<sup>1</sup>

<sup>1</sup>Diagnostic Imaging and Nuclear Medicine, Kyoto University Graduate School of Medicine, Kyoto, Kyoto, Japan, <sup>2</sup>Neurospin, CEA Saclay, Gif-sur-Yvette, Ile-de-France, France, <sup>3</sup>Kyoto University Faculty of Medicine, Kyoto, Kyoto, Japan, <sup>4</sup>Information Science and Technology, Osaka Institute of Technology, Hirakata, Osaka, Japan, <sup>5</sup>Siemens AG HIM MR PI Neuro, Erlangen, Erlangen, Germany

**Targeted audience:** Scientists and clinicians interested in perfusion MRI and breast cancer MRI

### Introduction

MR measurements based on motion encoding gradients, such as intravoxel incoherent motion (IVIM) imaging, could provide information on tissue microvasculature (e.g., flowing blood volume and blood velocity)<sup>1</sup>. It has been shown that IVIM MRI can provide valuable information on angiogenesis in cancer, including breast cancer<sup>2,3</sup>. A key feature of IVIM MRI is that it does not involve contrast agents, an alternative for perfusion MRI. Furthermore, as IVIM MRI relies on diffusion MRI additional information can be obtained on tissue structure. Here, we have evaluated the potential of IVIM and diffusion MRI for the diagnosis of breast tumors.

### Material and Methods

This study included 23 patients suspected of breast tumors (16 malignant and 7 benign tumors).

Breast MRI was performed using a 3-T system (Trio, B17; Siemens AG) equipped with a dedicated 16-channel breast array coil. The following images were obtained after localizers were acquired: 1. bilateral fat-suppressed T2-weighted images 2. Diffusion-weighted images (single shot EPI along three orthogonal axes; b values of 0, 5, 10, 20, 30, 50, 70, 100, 200, 400, 600, 800, 1000, 1500, 2000, 2500 sec/mm<sup>2</sup>; repetition time/echo time, 4,600/86 ms; flip angle, 90°; field of view, 160 × 300 mm<sup>2</sup>; matrix, 80 × 166; slice thickness, 3.0 mm; and acquisition time, 3 min 55 sec); 3. Dynamic contrast (DCE) images :non-fat-suppressed T1-weighted images; and fat-suppressed T1-weighted dynamic contrast-enhanced images obtained using a 3-dimensional fat-suppressed gradient-echo sequence (repetition time/echo time, 3.7/1.36 ms; flip angle, 15°; field of view, 330 × 330 mm<sup>2</sup>; matrix, 346 × 384; slice thickness, 1 mm; and acquisition time, 60 s). The fat-suppressed T1-weighted dynamic contrast-enhanced images were acquired before and 3 times (0–1, 1–2, and 5–6 min) after contrast injection. The signal attenuation curve was first fitted using a monoexponential diffusion model, and an ADC was estimated for each slice on a voxel-by-voxel basis by fitting the MRI signal against the b-values between 400 and 2500 sec/mm<sup>2</sup>. The diffusion component was then subtracted from the signal and the remaining signal was fitted using the IVIM model [1] for b values lower than 200 sec/mm<sup>2</sup> to get estimates of the flowing blood fraction,  $f_{IVIM}$ , and pseudodiffusion,  $D^*$  (Fig.1,2). For DCE, the initial enhancement (CE (%)) was calculated by;  $(SI_{0-1} - SI_{pre}) / SI_{pre}$  (SI; signal intensity), similar to a previous study<sup>3</sup>. ROIs were drawn manually based on the IVIM, ADC and DCE images for each patient, and the corresponding mean and standard deviation (%) of each parameter within the ROIs were derived for statistical analysis.

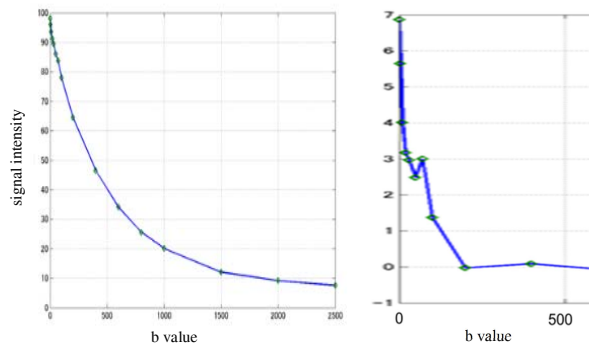


Figure 1; the signal decay Figure 2; remaining  $f_{IVIM}$  below 200 s/mm<sup>2</sup>

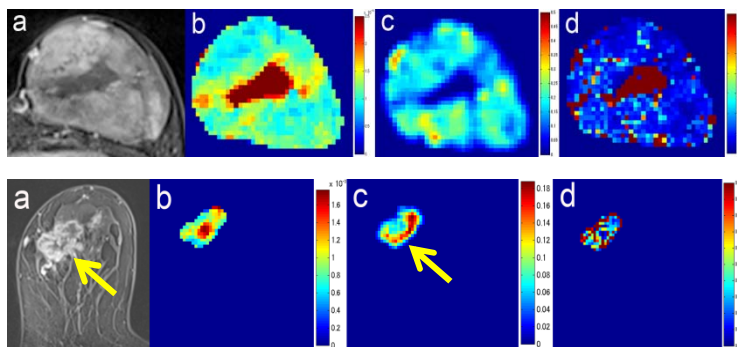


Figure 3,4 (a) initial CE T1W image (b) ADC map (c)  $f_{IVIM}$  map (d)  $D^*$  map.

Yellow arrows for figure 3a and 3c indicate the corresponding highly enhanced lesion and high IVIM fraction area respectively.

tumor and normal breast tissue. The ADC in malignant tumors was significantly lower than that of benign tumor ( $p=0.01$ ) and normal breast tissue ( $p=0.01$ ). Interestingly, the correlation between CE and  $f_{IVIM}$  was significant in normal breast tissue with a Pearson's coefficient ( $r$ ) of 0.55. One case of PASH (Pseudoangiomatous stromal hyperplasia) is shown in Fig.3. The IVIM map clearly delineates a central high area on T2-weighted image, with very low perfusion. Initial contrast enhancement and  $f_{IVIM}$  are much higher in the periphery of the lesion (Fig.1). In Fig.4 (malignant invasive ductal carcinoma) the high IVIM fraction area corresponds to the highly enhanced lesion (Fig.4, yellow arrows).

Although those preliminary results need to be validated at a broader scale, they suggest that images of blood microvasculature can be obtained without contrast agents using IVIM MRI. In combination with the ADC, the flowing blood fraction,  $f_{IVIM}$ , may help improve diagnostic accuracy of IVIM-MRI in breast cancer.

### References:

1. Le Bihan D, Breton E, Lallemand D, et al. Separation of diffusion and perfusion in intravoxel incoherent motion MR imaging. *Radiology*. 1988;168(2):497-505.
2. Luciani A, Vignaud A, Cavet M, et al. Liver cirrhosis: intravoxel incoherent motion MR imaging--pilot study. *Radiology*. 2008;249(3):891-899.
3. Sigmund E, E, G. Y. Cho, S. Kim, et al. Intravoxel incoherent motion imaging of tumor microenvironment in locally advanced breast cancer. *MRM* 2011;65:1437-1447.

Parameters	Malignant	Benign	Normal
ADC ( $10^{-3}$ mm <sup>2</sup> /sec)	0.98 ( $\pm 0.22$ )	1.53 ( $\pm 0.44$ )	1.77 ( $\pm 0.12$ )
$f_{IVIM}$ (%)	13.6 ( $\pm 2.2$ )	12.5 ( $\pm 5.1$ )	9.6 ( $\pm 2.9$ )
$D^*$ ( $10^{-3}$ mm <sup>2</sup> /sec)	6.8 ( $\pm 1.2$ )	7.1 ( $\pm 2.4$ )	8.3 ( $\pm 2.2$ )
CE (%)	165 ( $\pm 41$ )	94 ( $\pm 46$ )	13 ( $\pm 5$ )

Table 1: The mean values and the standard deviations derived from IVIM analysis and the initial enhancement.

### Results and Discussion

The IVIM parameters and the initial enhancement across malignant, benign tumor and normal breast tissue are summarized in Table 1. In malignant tumors  $f_{IVIM}$  was significantly ( $p=0.01$ ) higher than in the normal breast and showed a weak negative correlation with  $D^*$  with a Pearson's coefficient ( $r$ ) of -0.42.

However, there was no significant difference in  $f_{IVIM}$  between malignant and benign tumors. There was no significant difference in  $D^*$  across malignant, benign,